

Soft Matter

Accepted Manuscript



This is an *Accepted Manuscript*, which has been through the Royal Society of Chemistry peer review process and has been accepted for publication.

Accepted Manuscripts are published online shortly after acceptance, before technical editing, formatting and proof reading. Using this free service, authors can make their results available to the community, in citable form, before we publish the edited article. We will replace this *Accepted Manuscript* with the edited and formatted *Advance Article* as soon as it is available.

You can find more information about *Accepted Manuscripts* in the [Information for Authors](#).

Please note that technical editing may introduce minor changes to the text and/or graphics, which may alter content. The journal's standard [Terms & Conditions](#) and the [Ethical guidelines](#) still apply. In no event shall the Royal Society of Chemistry be held responsible for any errors or omissions in this *Accepted Manuscript* or any consequences arising from the use of any information it contains.

ARTICLE

Particle-size Dependent Melt Viscosity Behavior and Properties of Three-arm Star Polystyrene/Fe₃O₄ Composites

Cite this: DOI: 10.1039/x0xx00000x

Received 00th January 2012,

Accepted 00th January 2012

DOI: 10.1039/x0xx00000x

www.rsc.org/Haiying Tan,^{a,b} Yichao Lin,^{a,b} Jun Zheng,^{a,b} Jiang Gong,^{a,b} Jian Qiu,^a Haiping Xing,^{a,*} Tao Tang^{a,*}

The melt viscosity of three-arm star polystyrene (S3PS)/Fe₃O₄ nanoparticle composites was studied by means of rheological measurements. The arm molecular weight (M_a) of S3PS (or radius gyration) and particle size of Fe₃O₄ (radius (R_p): 3 nm and 44 nm) showed a strong influence on the melt viscosity behavior (at low shear frequencies) of S3PS/Fe₃O₄ composites. The reinforcement (viscosity increase) was observed in the composites where the M_a was higher than the M_c of PS (M_c : the critical molecular weight for chain entanglement). For $M_a < M_c$, when the size of Fe₃O₄ nanoparticle was changed, the melt viscosity of the composites exhibited either plasticization (melt viscosity reduction) or reinforcement. When the content of Fe₃O₄ was low (1 wt%), the transformation from plasticization to reinforcement behavior could be observed, which strongly depended on the size ratio of the radius of gyration (R_g) for S3PS to the size of nanoparticles (R_p). In addition, magnetic properties and thermal stability of S3PS/Fe₃O₄ composites were studied.

Introduction

Recently it has been found that the assembly of spherical nanoparticles in polymer matrices causes the reduction of melt viscosity¹⁻⁵. This phenomenon is in contradiction with the expression derived from Einstein⁶, describing the increase of the viscosity as a function of the volume fraction of fillers in a matrix. Mackay's group¹⁻³ has found that polymer molecular weight (M_w), radius of gyration (R_g) and nanoparticle radius (R_p), are key structural factors affecting the dispersion states of nanoparticles¹. The critical molecular weight for entanglement (M_c) designates where a viscosity reduction is possible.^{2,7} The average interparticle half-gap (h) and the ratio of R_g to R_p are also important for a viscosity decrease to occur. The h can be calculated from the following relationship:

$$h/R_g = [\phi_m/\phi]^{1/3} - 1 \quad (\text{Equation 1})$$

where ϕ_m is the maximum random packing volume fraction (~0.638), ϕ is the volume fraction of nanoparticles. Twice of this distance is the average distance separating particles. According to the results from Mackay group¹⁻³, viscosity reduction just happened when molecular weight of polymer was larger than the entanglement molecular weight and the h was smaller than R_g . Recently, a lot of attention has been paid on this phenomenon coming up with controversial observations and explanations.^{1-5,8-14} The possible mechanisms for the reduction of melt viscosity of polymer/nanoparticle composites include dilution of the entanglement density of polymer

chains⁵, increased excluded free volume induced around the nanoparticles,^{2,3} selective adsorption of high molecular weight polymer chains¹⁵, slip between sample and geometry during rheological testing⁷, constraint release of entangled polymer chain^{2,3,14}, and degradation of polymer^{16,17}.

So far the reduction of melt viscosity induced by the addition of the nanoparticles has been found in linear polymer matrix. Very recently, we have found that the presence of well-dispersed C₆₀ nanoparticles reduces the viscosity of star polystyrene (SPS) melts when the arm molecular weight (M_a) of SPS is smaller than the M_c of PS.¹⁸ However, the viscosity increases when the M_a is higher than M_c . The incorporation of POSS also decreases the melt viscosity of the unentangled SPS, and reinforces the polymer matrix when M_a is higher than M_c ¹⁹, although the interaction between POSS and SPS is different from that between C₆₀ and SPS. Importantly the R_p s of both C₆₀ and POSS are smaller than the R_g of SPS. Mackay's group studied the dependence of melt viscosity on the nanoparticle size and the average interparticle half-gap (h) in linear PS (LPS). They found that larger particle sizes will not produce melt viscosity decreased behaviour in entangled LPS.¹ However, there is no report studying the effects of the sizes of nanoparticles on the melt behavior of star polymer/nanoparticle systems.

In this work, following our previous study, two kinds of magnetic Fe₃O₄ nanoparticles with different diameters were used to explore the influence of the size of nanoparticles on the melt behavior of SPS/Fe₃O₄ composites. Magnetic polymer composites have attracted much attention because of their intriguing properties.²⁰⁻²⁴ The required properties to magnetic

nanoparticles for many applications are narrow nanosized distribution, high and uniform magnetic content and high saturation magnetization (M_s). Different applications require them to have different sizes. Owing to the need of applications, various methods were established to synthesize different sized Fe_3O_4 .^{21,23-25} Here two sizes of Fe_3O_4 were synthesized using the reported methods.^{21,25} The dependence of melt viscosity of SPS/ Fe_3O_4 composites on the M_w and R_g of SPS, the R_p of nanoparticle and the average interparticle half-gap (h) was studied. Also the influence of dispersed spherical nanoparticles in SPS matrix on thermal stability and magnetic performance of SPS was investigated.

Experimental Section

Materials. 1,3,5-tribromomethylbenzen and copper bromide (CuBr , 99.999%) were purchased from Aldrich. 2,2'-Dipyridyl was purchased from TCI. Styrene (99%), toluene, tetrahydrofuran (THF), CH_2Cl_2 , hexane, methanol, $\text{FeCl}_3 \cdot 6\text{H}_2\text{O}$, oleic acid, ethylene glycol (EG), ethylenediamine (EN), sodium acetate (NaAc), and neutral alumina were purchased from China National Medicines Corporation Ltd. $\text{Fe}(\text{acac})_3$, 1,2-hexadecanediol, phenyl ether and oleylamine were purchased from Acros. Styrene was distilled over CaH_2 prior to use. Toluene was purified by Braun system. All the other reagents were used as received. Three-arm star polystyrene (S3PS) was synthesized via ATRP technique. The details about the synthesis and characterization of S3PS samples were reported in our previous report¹⁸. Table 1 shows molecular parameters of a series of S3PS samples.

Table 1. Structure information of three-arm PS (S3PS) from triple detection size exclusion chromatography (SEC-MALLS)

Sample	M_w^a (kDa)	PDI	M_a^b (kDa)	R_g (nm)
S3PS-18k	18.5	1.18	6.2	3.1
S3PS-48k	48.2	1.13	16.0	5.3
S3PS-75k	74.9	1.13	25.0	8.7
S3PS-150k	150.0	1.66	64.9	13.5

^a Molecular weight of the arm (M_a) of star PS was determined by the relationship $M_a = 1/3M_w$ in S3PS.

Synthesis of nano- Fe_3O_4 (6 nm, named Fe(3)). Fe_3O_4 nanoparticles with the diameter of 6 nm were prepared according to the method of Sun.²⁵ $\text{Fe}(\text{acac})_3$ (2 mmol), 1,2-hexadecanediol (10 mmol), oleic acid (6 mmol), oleylamine (6 mmol), and phenyl ether (20 mL) were mixed and magnetically stirred under a flow of nitrogen. The mixture was heated to 200 °C for 30 min and then, under a blanket of nitrogen, heated to reflux (280 °C) for another 30 min. The black-brown mixture was cooled to room temperature by removing the heat source. Under ambient conditions, ethanol (40 mL) was added to the mixture, and a black material was precipitated and separated via centrifugation. The black product was dissolved in hexane in the presence of oleic acid (0.05 mL) and oleylamine (0.05 mL). Centrifugation (6500 rpm, 10 min) was applied to remove any undispersed residue. The product (Fe_3O_4 nanoparticles) was then precipitated with ethanol, centrifuged (6500 rpm, 10 min) to remove the solvent, and redispersed into hexane.

Synthesis of nano- Fe_3O_4 (88 nm, named Fe(44)). For the synthesis of 100 nm Fe_3O_4 nanoparticles, $\text{FeCl}_3 \cdot 6\text{H}_2\text{O}$ (2.50 g) was injected into a mixture containing 8.9 mL EN and 80 mL EG under magnetic stirring, followed by the addition of NaAc (5.00 g). The mixture was transferred to a Teflon-lined stainless-steel autoclave and sealed, to heat at 210 °C for 6 h.

The produced magnetite nanoparticles were washed with deionized water. The product, Fe_3O_4 nanoparticles with the diameter of 88 nm, was separated using a magnet, and finally dried in an oven at 80 °C for 12 h. This method was reported previously²¹.

Preparation of SPS/ Fe_3O_4 composites. Fe_3O_4 was dissolved in toluene at a concentration of 2 mg/mL by ultrasonic. Next, a certain amount of Fe_3O_4 /toluene solution was added to SPS/toluene solution to obtain the desired weight fractions of Fe_3O_4 in the final composite. The mixed solutions were dispersed by ultrasonic and then added drop-wise into a large volume of methanol to get co-precipitation of SPS and Fe_3O_4 . The solids were filtered from methanol and dried in vacuum at 80 °C for more than 24 h to remove the solvent. The symbol S3PS- x -Fe(y)- z represents three-arm star polystyrene/ Fe_3O_4 composites, here x is the molecular weight of S3PS, y represents the diameter (nm) of Fe_3O_4 nanoparticles and weight fraction of z Fe_3O_4 . To our best knowledge, large concentrations of particles will lead to aggregation, so the weight fraction of Fe_3O_4 in the polymer matrix was only 1 wt%.

Characterization. Dispersion state of the obtained SPS/ Fe_3O_4 composites was observed by transmission electron microscopes (TEM, JEOL1011 JEOL, Japan) and high resolution transmission electron microscope (Tecnai G2 F20 FE-TEM, FEI, Holland) on microtome sections at 100 kV and 200 kV accelerating voltage, respectively. Ultrathin sections were cut on Leica Ultracut using a glass knife at room temperature. The samples were collected on carbon-coated copper TEM grids. The glass transition temperature (T_g) of samples was measured by differential scanning calorimetry (DSC, Mettler Toledo DSC 1, Switzerland). Samples of about 10 mg were loaded in aluminum pans and heated at a rate of 10 °C min^{-1} under nitrogen atmosphere. A first scanning was carried out from room temperature to 200 °C and the samples were held for 3 min at this temperature to erase previous unknown thermal history. Then the samples were cooled down to ambient temperature and a second heating scan was carried out heating up to 200 °C. The temperature corresponding to the midpoint in the heat capacity step-rise was used for the determination of T_g . Thermal gravimetric analyses (TGA) were done using a Thermal Analysis Instrument (SDTQ600, TA Instruments). The mass losses of the dried samples were carried out under air atmosphere at 100 mL min^{-1} with a heating rate of 10 °C min^{-1} from room temperature to 800 °C. The rheological properties of samples were performed on a strain-controlled rheometer (ARES-G2, TA Instruments) using a plate-plate geometry (25 mm diameter). The temperature was controlled by a forced convection oven (FCO) unit under a nitrogen gas purge to minimize the degradation of the samples. A strain amplitude sweep (0.01–100 %) at a fixed frequency ($\omega = 1$ rad/s) was performed to establish the linear viscoelastic regime. Oscillatory frequency sweeps were performed from 0.05 to 200 rad/s with a strain in the linear regime. Flow sweeps were performed from 10^{-4} to 10 s $^{-1}$. Experimental temperature was 150 °C without other specification. Magnetization measurements were carried out with a superconducting quantum interface device (SQUID) magnetometer (Quantum Design MPMS XL) at 300 K with fields up to 1.0 T.

Results and discussion

Morphology of S3PS/ Fe_3O_4 composites. Fig. 1 shows the TEM images of synthesized Fe_3O_4 nanoparticles (Fe(3) and

Fe(44)) and their size distribution histograms. The average radii of Fe(3) and Fe(44), measured by Nano Measurer 1.2, were 3.2 and 43.7 nm, respectively. Based on the preparation method, the synthesised Fe_3O_4 was decorated by organic group as shown in Fig. S1. The size distribution of Fe(3) was narrower than that of Fe(44), which was caused by the different preparation methods. Fig. 1b was the HR-TEM image of Fe(3). The morphologies of SPS/ Fe_3O_4 composites were shown in the SI (Fig. S2). Most of both the particles could be dispersed in the matrices of S3PS-48k and S3PS-150k, although some of them formed aggregates. Considering their different sizes of the two particles, there was no obvious difference in the dispersion states.

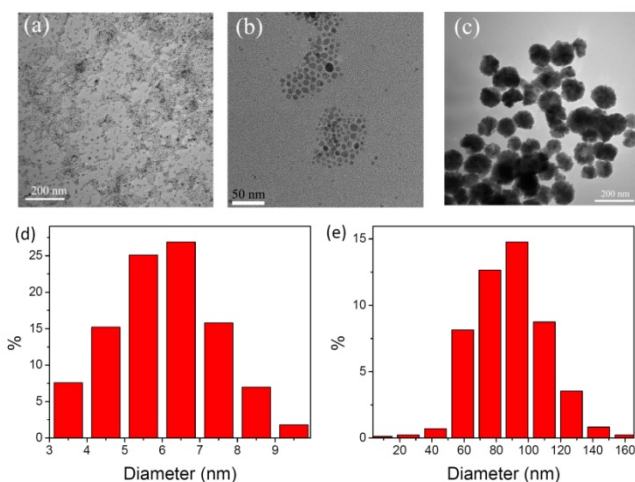


Fig. 1. Morphology of Fe_3O_4 synthesized by the two different methods. (a) TEM image of Fe(3) observed by TEM with the accelerate voltage at 100 kV; (b) TEM image of Fe(3) observed by HR-TEM with the accelerate voltage at 200 kV; (c) TEM image of Fe(44) observed by TEM with the accelerate voltage at 100 kV; size distribution of (d) Fe(3) and (e) Fe(44) was measured by Nano Measurer 1.2, respectively.

The effect of particle sizes on the melt viscosity. The influence of the added Fe_3O_4 on the melt behavior of S3PS was studied by linear oscillatory frequency sweep experiments. Fig. 3a shows the plots of complex viscosity (η^*) versus angular frequency (ω) for S3PS-18k containing Fe_3O_4 nanoparticles with two different sizes. The R_g of S3PS-18k (3.1 nm) was very close to the R_p (3.2 nm) of Fe(3) and smaller than that of Fe(44). Compared to pure S3PS-18k, the addition of these two Fe_3O_4 increased the η^* at low frequencies of S3PS-18k matrix. The changing trends of G' and G'' were similar to those of the η^* (Fig. S3). Large particles (Fe(44)) resulted in more increment in the η^* than that caused by small particles (Fe(3)). When the molecular weight of S3PS matrix was increased to 48k, the R_g of S3PS-48k (5.3 nm) was higher than the R_p of Fe(3) but lower than that of Fe(44). In this case, the incorporation of Fe(3) decreased the complex viscosity of S3PS-48k, but the presence of Fe(44) still increased the viscosity of S3PS-48k (Fig. 2b). Similar changing trend was observed in the melt viscosity for S3PS-75k, that is, the incorporation of Fe(3) decreased the η^* , the addition of Fe(44) increased the η^* (Fig. 2c). The R_g of S3PS-75k was 8.7 nm, which was higher than the R_p of Fe(3) but lower than that of Fe(44). It can be found that, when the polymer chains were unentangled ($M_a < M_c$, M_c of PS melt is about $\sim 34\text{kDa}$ ^{2,26}), the presence of large particles ($R_p > R_g$) reinforced polymer matrix, but small particles ($R_p < R_g$) decreased the η^* . Changing trends

of G' and G'' were similar to those of complex viscosity for S3PS-48k, S3PS-75k and their composites with Fe_3O_4 of two sizes (Fig. S4 and S5). Although the M_a s of S3PS-18k, S3PS-48k and S3PS-75k were smaller than the M_c of PS, the changing trends in the η^* of their composites were different, resulting from the different ratio of the R_g to the R_p of Fe_3O_4 nanoparticles. When the M_a of S3PS was higher than the M_c , the incorporation of Fe(3) or Fe(44) increased the viscosity of polymer matrix (Fig. 2d), no matter what the ratio of R_p to R_g was. Because the R_g of S3PS-150k was 13.5 nm, higher than R_p of Fe(3) but lower than R_p of Fe(44). The changing trends in G' and G'' for S3PS-150k and its composites with Fe(3) and Fe(44) were given in Fig. S6.

According to the summary made by Mackay group³, for a viscosity reduction in linear polymer composites: the polymer must be entangled ($M_w > M_c$), the radius of nanoparticle and the average interparticle half-gap (h) must be less than the R_g of polymer matrix. In this work, the radius of Fe(3) and Fe(44) (R_p) were 3.2 and 43.7 nm, respectively. The R_p of Fe(44) was larger than the R_g of all the synthesized S3PS (2.9–13.5 nm), but the R_p of Fe(3) was in between the R_g of the synthesized SPS, depending on the molecular weight of S3PS matrix. The value of interparticle half-gap (h) can be determined from the Equation 1 in the introduction part. In the samples with 1 wt% Fe_3O_4 , the h is 18.5 nm and 253.1 nm for Fe(3) and Fe(44) system, respectively. This shows that h values of both particles in S3PS/ Fe_3O_4 composites are larger than the R_g of all the synthesized S3PS (2.9–13.5 nm) (see Table 1), including the S3PS samples with $M_a < M_c$ and $M_a > M_c$. However, from the results in Fig. 2, different changing trend in complex viscosity was observed in the S3PS/ Fe_3O_4 composites. For example, the incorporation of Fe(3) increased the complex viscosity of S3PS-18k and S3PS-150k, but decreased the viscosity of S3PS-48k and S3PS-75k. So we guess that the Mackay's assumption that h must be lower than R_g , is not valid in this system. There are several other factors that might be responsible for the viscosity change in polymer matrix, which will be discussed in the later section.

To confirm the results about the changing trend of melt viscosity from linear frequency sweep measurements, flow sweep mode was also used in the rheological measurements. S3PS-48k and S3PS-150k were used as examples to show the changing trend of shear viscosity (η) versus shear rate ($\dot{\gamma}$). As shown in Fig. 3, S3PS-48k, S3PS-150k and their composites exhibit a Newtonian plateau region at low shear rate. The zero shear viscosity (η_0) could be directly obtained from the plateau at the lowest shear rate. The results of other samples were given in the SI (Fig. S7). Table 2 shows the η_0 of four kinds of S3PS and their composites with Fe_3O_4 . The incorporation of Fe(3) decreased the shear viscosity of S3PS-48k, but the presence of Fe(44) increased that of S3PS-48k (Fig. 3a). In contrast, the addition of both Fe(3) and Fe(44) increased the viscosity of the S3PS-150k (Fig. 3b). The larger the particle size, the higher the shear viscosity. The changing trend of shear viscosity for S3PS/ Fe_3O_4 composites was similar to that of complex viscosity of all the samples. On using the data of linear oscillatory frequency sweep experiments and steady shear rheology, Cox–Merz¹⁹ rules was tried. The so called Cox–Merz rule describes the relationship between complex viscosity and shear viscosity as:

$$\eta^*(\omega)|_{\omega \rightarrow 0} = \eta(\dot{\gamma})|_{\dot{\gamma} \rightarrow 0} \quad (\text{Equation 2})$$

But for some of the samples it failed, e.g. S3PS-150k-Fe(44), which results from the aggregation formed (Fig S2d). The failure of the Cox–Merz rule for these composites (while being

obeyed for the polymer itself) suggests aggregates formed in the composites.²⁷ In SPS/Fe₃O₄ composites, the formation of

large aggregates was responsible for the failure of this rule.

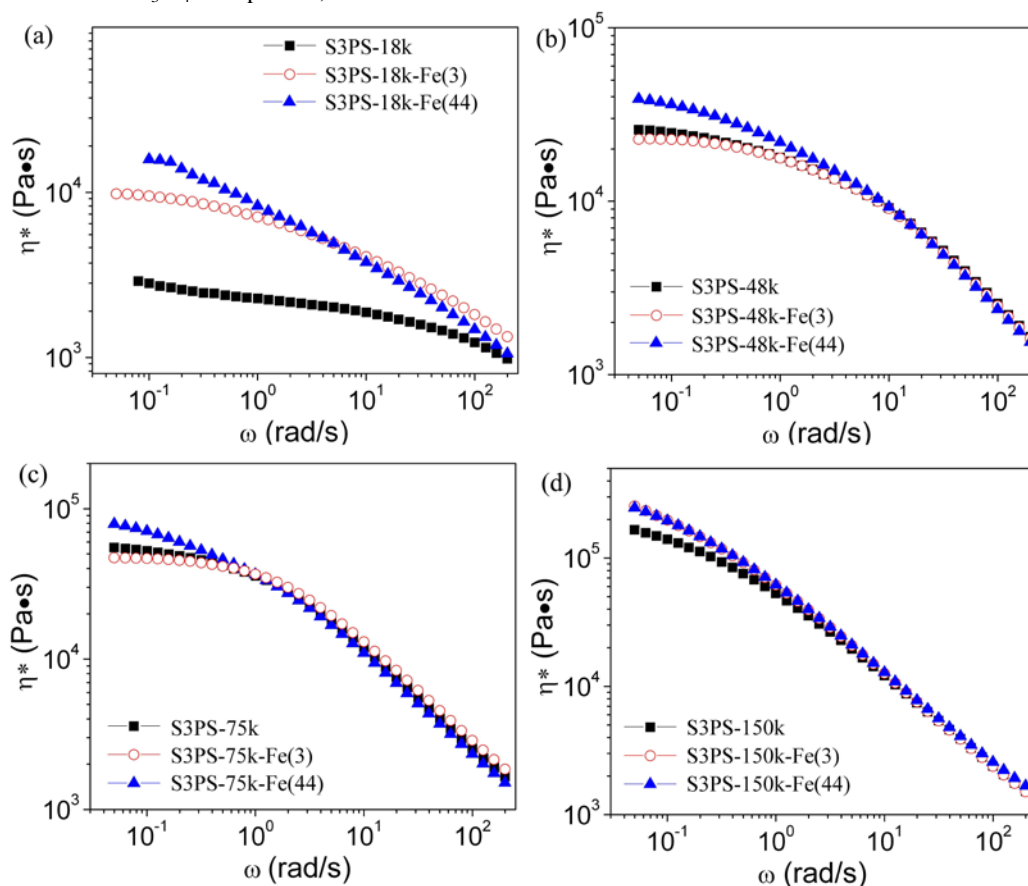


Fig. 2. Complex viscosity (η^*) vs angular frequency (ω) for (a) S3PS-18k, (b) S3PS-48k, (c) S3PS-75k, (d) S3PS-150k and their composites with two different sizes of Fe₃O₄ at 150 °C.

Table 2. The glass transition temperature (T_g), plateau modulus (G_N^0), apparent relaxation time (τ_a), zero shear viscosity (η_0) and $\eta_{0.05}^*$ for pure S3PS and their composites with Fe₃O₄ nanoparticles

Sample	T_g (°C)	G_N^0 (MPa)	τ_a (s) ^a	η_0 ^b (Pa·s)	$\eta_{0.05}^*$ ^c (Pa·s)
S3PS-18k	99.2±0.3	--	--	3100±100	2900±100
S3PS-18k-Fe(3)	102.3±0.1	--	--	13100±600	9780±400
S3PS-18k-Fe(44)	102.2±0.2	--	0.006	40800±1600	20100±400
S3PS-48k	101.9±0.3	0.22±0.02	0.045	38900(±1200)	25800(±900)
S3PS-48k-Fe(3)	103.4±0.4	0.22±0.04	0.043	28800±1100	22700±1100
S3PS-48k-Fe(44)	103.6±0.2	0.16±0.01	0.074	47700±1000	38900±1200
S3PS-75k	104.1±0.2	0.17±0.01	0.242	55800±2700	55100±1100
S3PS-75k-Fe(3)	103.9±0.1	0.19±0.03	0.203	38900±1400	47200±1500
S3PS-75k-Fe(44)	103.5±0.3	0.15±0.02	0.364	101200±3500	78000±2100
S3PS-150k	105.8±0.2	0.15±0.03	1.248	166500±2300	165000±2500
S3PS-150k-Fe(3)	105.1±0.3	0.13±0.02	3.096	379200±1800	251400±1100
S3PS-150k-Fe(44)	102.5±0.4	0.12±0.04	3.646	685500±1100	254400±1200

^a The relaxation time was determined from the relationship: $\tau_a = 1/\omega_{\text{cross}}$, where ω_{cross} was the angular frequency where the storage modulus equals to loss modulus showed in Table S1. ^b Zero shear viscosity determined from the plateau region of steady state shear viscosity. ^c complex viscosity at the frequency of 0.05 rad/s.

ARTICLE

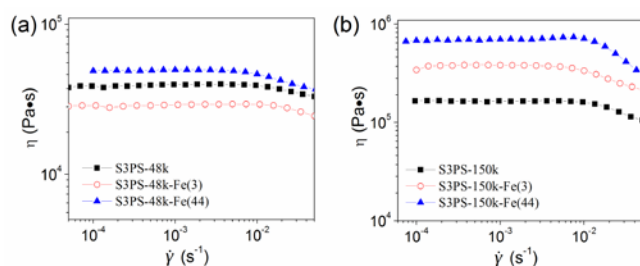


Fig. 3. Steady state shear viscosity as a function of shear rate for (a) S3PS-48k and (b) S3PS-150k and their composites with 1 wt% of Fe(3) and Fe(44) at 150 °C.

Fig. 4 shows the ratio of viscosity ratio ($\eta_{0.05,C}^*$ to $\eta_{0.05,P}^*$) as a function of R_g/R_p . For the composites containing both Fe(3) and Fe(44), when the arm molecular weight was smaller than the M_c , the viscosity ratio decreased with the increase of R_g/R_p . However, it increased when the M_a was higher than M_c , although the R_g/R_p ratio became larger. The main difference in the viscosity ratio changing was that the viscosity ratio became lower than 1 when $M_a < M_c$ and $R_g/R_p > 1$. It can be seen that the viscosity ratio depends on both the arm molecular weight and the R_g/R_p ratio.

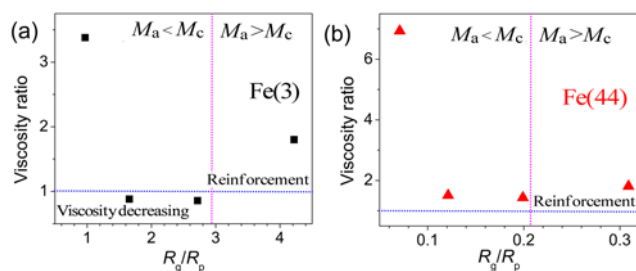


Fig. 4. Viscosity ratio ($\eta_{0.05,C}^*/\eta_{0.05,P}^*$) versus R_g/R_p for the composites containing Fe(3) and Fe(44) ($\eta_{0.05,C}^*$: the complex viscosity at 0.05 rad/s for S3PS/Fe₃O₄ composites; $\eta_{0.05,P}^*$: the complex viscosity at 0.05 rad/s for pure S3PS).

From the oscillatory frequency sweep results, the plateau modulus (G_N^0) of a sample is obtained by the “MIN method”²⁸.

$$G_N^0 = G'(\omega)_{\tan\delta \rightarrow \min}$$

where $\tan\delta$ is the damping factor, and the value of G' at the minimum of $\tan\delta$ is G_N^0 . The apparent relaxation time (τ_a) of the sample is calculated from the cross-over frequency (ω_c) of G' and G'' from the linear frequency sweep results ($\tau_a = 1/\omega_c$).¹⁴ The G_N^0 , τ_a and $\eta_{0.05}^*$ of the samples are summarized in Table 1. The changing trend of $\eta_{0.05}^*$ of S3PS/Fe₃O₄ composites was consistent with that of apparent viscosity (η_a , $\eta_a = G_N^0 \cdot \tau_a$).²⁹ Owing to the low complex viscosity of S3PS-18k, the ω_c of the samples cannot be determined under the measured conditions. The addition of Fe(3) slightly decreased the τ_a of S3PS-48k, but the presence of Fe(44) increased the τ_a of S3PS-48k. The τ_a of S3PS-75k showed a similar changing trend after incorporating

Fe₃O₄ nanoparticles. The changing trend of τ_a in both S3PS-48k and S3PS-75k matrices was similar to $\eta_{0.05}^*$. When the arm chain was entangled, the incorporation of both Fe(3) and Fe(44) increased the τ_a . The changing trend of τ_a for S3PS-150k was also similar to that of the complex viscosity. Thus the addition of Fe₃O₄ affected the relaxation mode of S3PS. Generally speaking, the addition of Fe₃O₄ decreased the G_N^0 of S3PS/Fe₃O₄ composites except the case of S3PS-75k-Fe(3). This result demonstrated that the addition of Fe₃O₄ changed the chain relaxation mode of S3PS matrix to some extent. Larger particles will block the chain relaxation process.

To further study the relaxation process of S3PS/Fe₃O₄ in large time scales, Fig. 5 shows the continuous relaxation spectra of S3PS-48k, S3PS-150k and their composites as examples. At a short time scale, the presence of Fe₃O₄ did not significantly affect the Rouse or the plateau regime in the relaxation spectra of S3PS-48k or S3PS-150k. Instead, at a longer time scale, the incorporation of Fe₃O₄ influenced the terminal region of the relaxation spectra of S3PS/Fe₃O₄ composites. Compared to the relaxation behavior of pure S3PS-48k, the longest relaxation time of S3PS-48k-Fe(3) became shorter, while the longest relaxation time of S3PS-48k-Fe(44) became longer (Fig. 5a). In Fig. 5b, the longest relaxation times of S3PS-150k/Fe₃O₄ composites were always longer than that of pure S3PS-150k matrix. These results were consistent with the changing trends of their melt viscosities at low shear frequencies (see Fig.S4b and S4d). Thus, the incorporation of Fe₃O₄ changed the relaxation mode of star PS chains. Large particles blocked the relaxation of S3PS chain, but small particles acted as lubricator that promoted the motion of the chains and resulted in decreased viscosity.

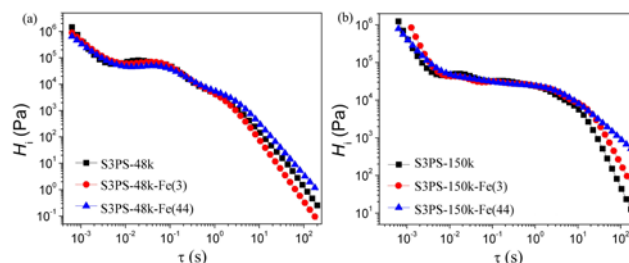


Fig. 5. Relaxation spectra for S3PS-48k (a) and S3PS-150k (b) with Fe(3) and Fe(44) at 150 °C.

Discussion about the changing trends of melt viscosity of S3PS/Fe₃O₄ composites. In our previous reports,^{18,19} the reduction of melt viscosity in the S3PS/C₆₀ (or POSS) system can be observed only in the S3PS matrix with low molecular weight ($M_a < M_c$) and the R_g of S3PS was higher than R_p . What will occur to the melt viscosity of S3PS when $R_g \leq R_p$? Unfortunately, the diameters of C₆₀ (0.7 nm) and POSS (1.5 nm) are always smaller than the R_g of all the synthesized SPS, and it is difficult to change the diameters of both them. So here we synthesize different sized Fe₃O₄ to study the influence of the size of nanoparticles on melt viscosity of S3PS. In this work, the results showed that the values of M_a , R_g and R_p determined the changing trend of melt viscosity for S3PS/Fe₃O₄ system. In

the cases with $M_a < M_c$, when $R_g > R_p$, the melt viscosity of S3PS/Fe₃O₄ (1 wt%) composites was lower than that of S3PS; however, when $R_g \leq R_p$, the increased melt viscosity was observed in the S3PS/Fe₃O₄ system. When M_a was higher than M_c , in spite of the ratio of R_g to R_p , the incorporation of Fe₃O₄ increased the complex viscosity of S3PS. Compared to our previous reports, we find that in this work, when $R_g \leq R_p$, the addition of Fe₃O₄ composites always increases the melt viscosity of S3PS in spite of the ratio of M_a to M_c . This can be explained by hydrodynamic reinforcement. The case of $R_g \leq R_p$ is similar to forming aggregates of small nanoparticles (such as the cases containing high content of C₆₀ or POSS), which results in hydrodynamic reinforcement for polymer melt. This proves that the basic requirement ($R_g > R_p$) for the appearance of the reduced melt viscosity is also necessary in the star polymer/nanoparticle composites.

In summary, there are several possible factors to influence the changing trend of melt viscosity in polymer/nanoparticles composites. Firstly, the topological structure was one of the main reasons for the dependence of melt viscosity of star polymer/nanoparticles system on the molecular weight of arms in star polymers. Owing to steric resistance, the nanoparticles can not enter the centre of star polymers, and most of nanoparticles are distributed the end regime of star polymers. So the topological structure of star polymer induces a more heterogeneous dispersion of nanoparticles in the star polymer matrix than the dispersion state of nanoparticles in the linear polymer matrix^{18,19,29,30}. Secondly, both $M_a < M_c$ and $R_g > R_p$ are the basic requirements for the appearance of the reduced melt viscosity in the star polymer/nanoparticle composites. Of course, the well-dispersed state of nanoparticles is also required. From the above results, it can be seen that the change of melt viscosity is only closely related to the relaxation time (Table 2), not to the G_N^0 and glass transition temperature (T_g). As we know, the free volume is tied up with the T_g of polymers. Generally, the increase of T_g means the reduction of the free volume. The presence of Fe(3) or Fe(44) increased the T_g of S3PS-48k, but the addition of Fe(3) decreased the melt viscosity of S3PS-48k, and the addition of Fe(44) led to the increase of melt viscosity of S3PS-48k. Comparing the change trend of melt viscosity with that of T_g in S3PS-75k and S3PS-150k before and after adding Fe₃O₄ nanoparticles, we also did not find their close relation.

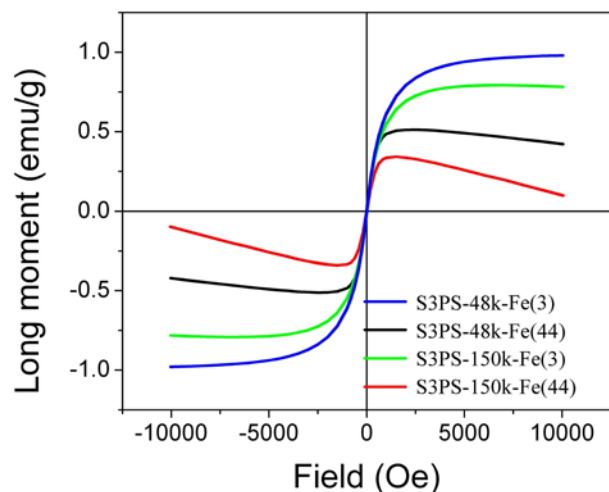


Fig. 6. Hysteresis loops of S3PS-48k-Fe(3), S3PS-48k-Fe(44), S3PS-150k-Fe(3) and S3PS-150k-Fe(44) at 300 K.

Magnetic properties. The magnetic properties of S3PS/Fe₃O₄ composites were examined at 300 K via a superconducting quantum interface device (SQUID) magnetometer. As revealed in the hysteresis loops (Fig. 6), the field dependent magnetization plot illustrates that the S3PS/Fe₃O₄ composites are superparamagnetic at room temperature, since there is no hysteresis detected, and both remanence and coercivity are approximately zero.³¹ The saturation magnetization values of Fe(3) and Fe(44) were 77.1 and 65.9 emu g⁻¹, respectively. The saturation magnetizations of S3PS/Fe(3) and S3PS/Fe(44) were less than those of Fe₃O₄ nanoparticles. As shown in Fig. 6, the saturation magnetizations of S3PS-48k-Fe(3) and S3PS-48k-Fe(44) were 0.97 and 0.51 emu g⁻¹, respectively; and those of S3PS-150k-Fe(3) and S3PS-150k-Fe(44) were 0.79 and 0.34 emu g⁻¹, respectively. In the cases containing Fe(3), there are large aggregates formed in S3PS-150k matrix, so the saturation magnetizations of S3PS-150k/Fe(3) composites was lower than that of S3PS-48k/Fe(3) composites. Comparing the saturation magnetizations of Fe(3) and Fe(44) with S3PS-48k, the larger the particle size, the smaller the value of saturation magnetizations. This might be attributed to the two factors: the saturation magnetizations for Fe(44) is lower than that of Fe(3). The incorporation of Fe₃O₄ endowed S3PS matrix with magnetic properties.

Table 3. Summary of the TGA results (Fig. 7) for S3PS-48k, S3PS-150k and their composites with Fe(3) and Fe(44) under air atmosphere.

Sample	$T_{5\text{wt}\%}$ (°C) ^a	$T_{10\text{wt}\%}$ (°C) ^a	T_{max} (°C) ^b
S3PS-48k	342	355	399
S3PS-48k-Fe(3)	354	370	416
S3PS-48k-Fe(44)	348	367	416
S3PS-150k	354	367	402
S3PS-150k-Fe(3)	368	377	418
S3PS-150k-Fe(44)	361	375	414

^a $T_{5\text{wt}\%}$ and $T_{10\text{wt}\%}$ are the temperature where 5 and 10 wt % weight loss occurred. ^b T_{max} equals to the temperature at which the maximum weight loss rate occurred.

Thermal stability. Fig. 7 presents TGA curves of S3PSs and their composites with Fe₃O₄ under air atmosphere. Detailed data are listed in Table 3. The temperature at 5 wt% weight loss ($T_{5\text{wt}\%}$) for S3PS-48k was lower than that of S3PS-150k, but the temperature for the maximum weight loss rate (T_{max}) of both S3PS-48k and S3PS-150k appears at ~400 °C, which is very close to that of linear PS.^{32,33} As for the S3PS-48k-Fe(3) composites, its $T_{5\text{wt}\%}$, $T_{10\text{wt}\%}$, and T_{max} were 12, 15, and 17 °C higher than those of pure S3PS-48k, indicating that the presence of Fe₃O₄ dramatically improved the thermooxidative stability of S3PS under air. As for Fe(44), similar changing trends in $T_{5\text{wt}\%}$, $T_{10\text{wt}\%}$ and T_{max} were observed. When the molecular weight of S3PS was increased to 150k, the $T_{5\text{wt}\%}$, $T_{10\text{wt}\%}$ and T_{max} of S3PS-150k-Fe(3) were 14, 10, 16 °C higher than those of S3PS-150k. Similar changing trends in $T_{5\text{wt}\%}$, $T_{10\text{wt}\%}$ and T_{max} of S3PS-150k-Fe(44) were also observed. The temperature for the maximum weight loss rate increased about 15 °C under air atmosphere. From these results, it is evident that the thermooxidative stabilities of all the S3PS/Fe₃O₄ composites were improved comparing with that of pure S3PS

matrix. Similar changing trend in S3PS-18k and S3PS-75k was observed.

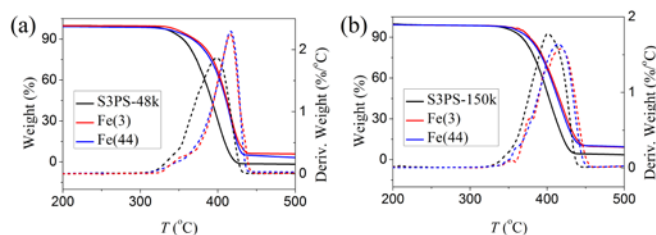


Fig. 7. TGA and DTG curves of (a) S3PS-48k, (b) S3PS-150k and their composites with Fe(3) and Fe(44) under air atmosphere.

Conclusions

Compared to pure S3PS, the melt behaviour of S3PS/Fe₃O₄ composites strongly depended on the molecular weight of arm (M_a) and the size of Fe₃O₄ nanoparticles (R_p). The incorporation of Fe₃O₄ changed the relaxation model of the S3PS chains, in which the longest relaxation time changed with the complex viscosity. When $R_g \leq R_p$, the addition of small amount of Fe₃O₄ nanoparticles (1 wt%) resulted in the increase in the melt viscosity of S3PS/Fe₃O₄ composites, in spite of molecular weight of arm in star PS. The reduced melt viscosity was observed in the S3PS/Fe₃O₄ composites, where $M_a < M_c$ and $R_g > R_p$. Interestingly, in the case of S3PS with low molecular weight ($M_a < M_c$), there was the crossover from plasticization (viscosity reduction) to reinforcement behavior (viscosity increase) by adjusting the size ratio of R_g of S3PS to nanoparticles size (R_p). This provides a new method to control melt behaviour of polymers. Furthermore, the addition of Fe₃O₄ nanoparticles also endowed the materials magnetic properties, and improved thermal stability of S3PS.

Acknowledgements

This work is financially supported by the National Natural Science Foundation of China for the Projects (51233005, 51073149 and 21304089).

Notes and references

^a State Key Laboratory of Polymer Physics and Chemistry, Changchun Institute of Applied Chemistry, Chinese Academy of Sciences, Changchun 130022, China

^b University of the Chinese Academy of Sciences, Beijing 100039, China
*Email: ttang@ciac.ac.cn; hpxing@ciac.ac.cn

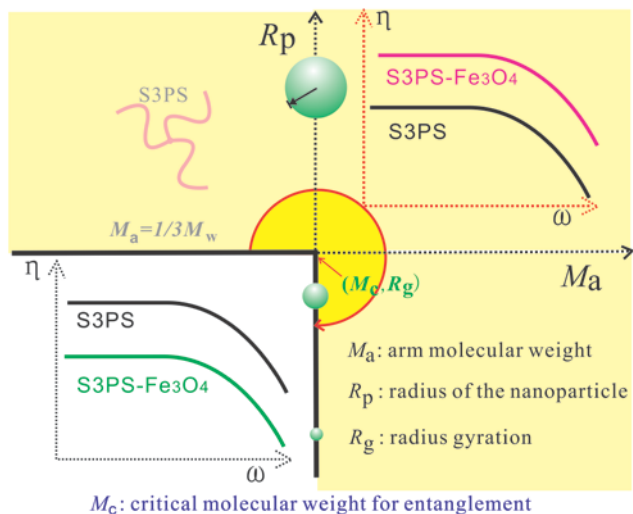
Electronic Supplementary Information (ESI) available: [details of any supplementary information available should be included here]. See DOI: 10.1039/b000000x/

- M. E. Mackay, A. Tuteja, P. M. Duxbury, C. J. Hawker, B. Van Horn, Z. Guan, G. Chen, R. S. Krishnan, *Science* 2006, **311**, 1740-1743.
- A. Tuteja, M. E. Mackay, C. J. Hawker, B. Van Horn, *Macromolecules* 2005, **38**, 8000-8011.
- A. Tuteja, P. M. Duxbury, M. E. Mackay, *Macromolecules* 2007, **40**, 9427-9434.
- R. G. Schmidt, G. V. Gordon, C. c. A. Dreiss, T. Cosgrove, V. J. Krukoni, K. Williams, P. M. Wetmore, *Macromolecules* 2010, **43**, 10143-10151.
- G. V. Gordon, R. G. Schmidt, M. Quintero, N. J. Benton, T. Cosgrove, V. J. Krukoni, K. Williams, P. M. Wetmore, *Macromolecules* 2010, **43**, 10132-10142.
- A. Einstein, *Ann. Phys.-Berlin* 1905, **17**, 549-560.
- M. E. Mackay, T. T. Dao, A. Tuteja, D. L. Ho, B. Van Horn, H.-C. Kim, C. Hawker, *Nat Mater* 2003, **2**, 762-766.
- A. C. Balazs, T. Emrick, T. P. Russell, *Science* 2006, **314**, 1107-1110.
- J. M. Kropka, K. W. Putz, V. Pryamitsyn, V. Ganesan, P. F. Green, *Macromolecules* 2007, **40**, 5424-5432.
- M. Mu, M. E. Seitz, N. Clarke, R. J. Composto, K. I. Winey, *Macromolecules* 2010, **44**, 191-193.
- J. A. Pomposo, A. R. de Luzuriaga, A. Etxeberria, J. Rodriguez, *Phys. Chem. Chem. Phys.* 2008, **10**, 650-651.
- Y. Li, M. Kröger, W. K. Liu, *Phys. Rev. Lett.* 2012, **109**, 118001.
- J. T. Kalathi, G. S. Grest, S. K. Kumar, *Phys. Rev. Lett.* 2012, **109**, 198301.
- D. Kim, S. Srivastava, S. Narayanan, L. A. Archer, *Soft Matter* 2012, **8**, 10813-10818.
- S. Jain, J. G. P. Goossens, G. W. M. Peters, M. van Duin, P. J. Lemstra, *Soft Matter* 2008, **4**, 1848-1854.
- J. W. Cho, D. R. Paul, *Polymer* 2001, **42**, 1083-1094.
- D. Schulze, S. Trinkle, R. Mülhaupt, C. Friedrich, *Rheol. Acta* 2003, **42**, 251-258.
- H. Tan, D. Xu, D. Wan, Y. Wang, L. Wang, J. Zheng, F. Liu, L. Ma, T. Tang, *Soft Matter* 2013, **9**, 6282-6290.
- H. Tan, J. Zheng, D. Xu, D. Wan, J. Qiu, T. Tang, *J. Phys. Chem. B* 2014, 5229-5239.
- F. Yan, J. Li, J. Zhang, F. Liu, W. Yang, *J. Nanopart. Res.* 2009, **11**, 289-296.
- G. Cheng, Y.-L. Liu, Z.-G. Wang, J.-L. Zhang, D.-H. Sun, J.-Z. Ni, *J. Mater. Chem.* 2012, **22**, 21998-22004.
- L. Fang, L. Ke-Xia, J. Wen, Z. Xiao-Bo, W. Yao, G. Zhong-Wei, *Nanotechnology* 2011, **22**, 225604.
- H. Xu, L. Cui, N. Tong, H. Gu, *J. Am. Chem. Soc.* 2006, **128**, 15582-15583.
- Z. L. Liu, Y. J. Liu, K. L. Yao, Z. H. Ding, J. Tao, Wang, X. J. *Mater. Synth. Proc.* 2002, **10**, 83-87.
- S. Sun, H. Zeng, D. B. Robinson, S. Raoux, P. M. Rice, S. X. Wang, G. Li, *J. Am. Chem. Soc.* 2003, **126**, 273-279.
- C. Liu, J. He, E. V. Ruymbeke, R. Keunings, C. Bailly, *Polymer* 2006, **47**, 4461-4479.
- T. Chatterjee, R. Krishnamoorti, *Soft Matter* 2013, **9** (40), 9515-9529.
- M. Rubinstein, R. H. Colby, *Polymer Physics*; Oxford University Press: New York, 2003.
- C. Tsenoglou, *Macromolecules*, 1991, **24**, 1762-1767.
- J. d. Cloizeaux, *Makromol. Chem. Makromol. Symp.*, 1991, **45**, 153-167.
- N. A. Frey, S. Peng, K. Cheng, S. H. Sun, *Chem. Soc. Rev.* 2009, **38**, 2532-2542.
- J. D. Peterson, S. Vyazovkin, C. A. Wight, *Macromol. Chem. Phys.* 2001, **202**, 775-784.
- I. C. McNeill, *Angew. Makromol. Chem.* 1997, **247**, 179-195.

For Table of Contents only

Particle-size Dependent Melt Viscosity Behavior and Properties of Three-arm Star Polystyrene/ Fe_3O_4 Composites

Haiying Tan,^{a,b} Yichao Lin,^{a,b} Jun Zheng,^{a,b} Jiang Gong,^{a,b} Jian Qiu,^a Haiping Xing,^{a,*} Tao Tang^{a,*}



Compared to three-arm star polystyrene (S3PS), the melt viscosity of S3PS/ Fe_3O_4 composites reduces (white area) or increases (yellow area), which strongly depends on arm molecular weight of S3PS (M_a), radius gyration of SPS (R_g) and the size of Fe_3O_4 nanoparticles (R_p).